

Mössbauer study on chemical short-range ordering during structural relaxation in $(\text{Co}, \text{Fe})_{75} \text{Si}_{10} \text{B}_{15}$ metallic glass

TAKAYUKI KOMATSU

Department of Chemistry, Nagaoka University of Technology, Nagaoka 940-21, Japan

The changes in the microscopic state of Fe-site surroundings during structural relaxation in a $(\text{Co}_{0.75}\text{Fe}_{0.25})_{75} \text{Si}_{10} \text{B}_{15}$ metallic glass which shows a remarkable reversible relaxation were examined using Mössbauer-effect measurements at 300 K. The narrowing of the distributions in the magnetic hyperfine field, H_i , and in the isomer shift, δ_{IS} , and the separation into two parts in the quadrupole splitting, Δ_{QS} , due to irreversible and reversible relaxations were clearly observed. A shift towards higher values in the mean H_i and a decrease in the mean δ_{IS} were also found in both relaxations. The features of the changes in H_i , δ_{IS} and Δ_{QS} strongly support the theory that the irreversible structural relaxation corresponds to topological short-range ordering which is mainly due to the ordering of Si and B atoms (that is, from random distributions to well-defined positions) and the theory that the reversible structural relaxation arises mainly from chemical short-range ordering between Co and Fe atoms.

1. Introduction

Structural relaxation is an extremely important phenomenon in amorphous materials. In metallic glasses, particularly, structural relaxation occurs not only at the glass-transition region but also at the low-temperature region well below the glass transition. Since the structural relaxation in metallic glasses results in a change in almost all the physical properties, such as magnetic and electrical properties, it is quite important to clarify the relaxation phenomenon in metallic glasses, especially the way in which actual atomic rearrangements in the glass structure correspond to the structural relaxation.

So far, it has been well established from various property changes that two types of structural relaxation occur during thermal annealing in metallic glasses, namely, irreversible relaxation and reversible relaxation. It should be pointed out that irreversible structural relaxation apparently occurs in all metallic glasses irrespective of their chemical compositions and it involves an increase of density, but reversible relaxation depends strongly on the chemical composition and involves no change in density; in particular reversible relaxation occurs remarkably in metallic glasses containing two or more kinds of transition-metal atoms such as Co–Fe–Si–B, Fe–Ni–Si–B or Co–Fe–Ni–Si–B [1–5]. To date, the concepts of topological short-range ordering (TSRO) for irreversible relaxation and chemical short-range ordering (CSRO) for reversible relaxation have been widely accepted (see, for example, [6–9]). However, there are still arguments about the applicability of the CSRO model to reversible structural relaxation in metallic glasses [10, 11]. Since the degree of the reversible structural relaxation in metallic glasses is usually very

small, very precise experimental techniques are required to clarify the mechanism of reversible structural relaxation. Direct structural evidence for reversible relaxation has been observed only in $\text{Pd}_{40}\text{Ni}_{40}\text{P}_{20}$ and $(\text{Mn}, \text{Ni})_{75}\text{P}_{16}\text{B}_6\text{Al}_3$ metallic glasses by using X-ray diffraction (XRD) or pulsed neutron scattering [12, 13], and it has been confirmed that reversible structural relaxation arises from atomic rearrangements. Similar results have not been reported for Co–Fe-based and Fe–Ni-based metallic glasses so far.

In the present study, we measured the Mössbauer spectra for as-quenched and annealed samples of $(\text{Co}_{0.75}\text{Fe}_{0.25})_{75} \text{Si}_{10} \text{B}_{15}$ metallic glass, and examined the changes in the microscopic state of Fe atoms to clarify the mechanism of structural relaxation, particularly in atomic rearrangements due to reversible structural relaxation. The compositional dependence (Co/Fe ratio) and kinetics of structural relaxation in Co–Fe–Si–B metallic glasses have been extensively studied by measuring the electrical resistivity changes by Komatsu *et al.* [1, 8, 14–17], and it has been proposed that reversible structural relaxation is attributed to reversible short-range ordering (SRO) between Co and Fe atoms depending on the annealing temperature. It has been found that the largest changes in resistivity due to reversible structural relaxation in $(\text{Co}_{1-x}\text{Fe}_x)_{75} \text{Si}_{10} \text{B}_{15}$ metallic glasses occurs in the $(\text{Co}_{0.75}\text{Fe}_{0.25})_{75} \text{Si}_{10} \text{B}_{15}$ composition with Co/Fe = 3; this means that this metallic glass would be very suitable in the study of the microscopic mechanism of reversible structural relaxation. We believe that the selection of metallic glasses is extremely important for the study of reversible structural relaxation, because the degree of the reversible structural

relaxation in metallic glasses is usually very small. Co-Fe-based metallic glasses are very important materials for technical applications because of their soft magnetic properties, and thus clarification of their structural-relaxation phenomenon has been strongly desired. Further, the Co-Fe-Si-B system is one of the most basic systems in transition-metal/metalloid metallic glasses.

The Mössbauer effect on ^{57}Fe is a powerful technique which is used to obtain information on very local surroundings of Fe atoms, both in amorphous and crystalline materials; and numerous papers have been written on the Mössbauer-effect measurements of various metallic glasses containing Fe atoms. Recently, Pilipczuk and Kopcewicz [18] have measured the Mössbauer spectra of $\text{Fe}_{74}\text{Co}_4\text{Si}_9\text{B}_{13}$ metallic glass and have found that annealing at 177°C for 40 min under a tensile stress causes a shift towards higher values in the magnetic hyperfine field of Fe atoms. These experiments gave information on the atomic arrangements due to the irreversible structural relaxation. To the author's knowledge, Mössbauer effects or XRD studies on reversible structural relaxation in Co-Fe-based metallic glasses have not been reported.

2. Experimental procedure

The $(\text{Co}_{0.75}\text{Fe}_{0.25})_{75}\text{Si}_{10}\text{B}_{15}$ metallic glass was prepared in the form of a ribbon, about $20\ \mu\text{m}$ and $1.5\ \text{mm}$ wide, by rapid quenching using a single-roller casting apparatus. The glass-transition, T_g , crystallization, T_x , and Curie temperatures, T_c , were determined by differential scanning calorimetry (DSC) at a heating rate of $30\ \text{K}\ \text{min}^{-1}$. The amorphous state of the samples was examined by XRD using $\text{CuK}\alpha$ radiation. The Mössbauer-effect measurements were carried out at $300\ \text{K}$ on the as-quenched samples and on some annealed samples. For the γ -ray source, a $10\ \text{mCi}$ in metallic Rh was used. The γ -rays were detected in a proportional counter filled with Xe and CO_2 gases. The velocity calibration was obtained from the six-line hyperfine spectrum of a pure-iron foil.

3. Features of the annealed samples

In order to study the irreversible- and reversible-structural-relaxation phenomena in metallic glasses, as-quenched samples had to be annealed at temperatures near and below the glass transition. In this study, the three samples listed below were used for the Mössbauer-effect measurements of $(\text{Co}_{0.75}\text{Fe}_{0.25})_{75}\text{Si}_{10}\text{B}_{15}$ metallic glass. The values of T_g , T_x and T_c of this as-quenched metallic glass were 480 , 530 and 523°C , respectively.

Sample A. The as-quenched metallic glass. In this sample, a frozen-in excess free volume is involved, and the arrangements among the constituent atoms would be largely random and distributed.

Sample B. The sample annealed at 475°C for 30 min. In this sample annealed near T_g , the irreversible structural relaxation is almost complete [1, 17].

Sample C. This sample was obtained by the following annealing procedure; the as-quenched glass was first annealed at 475°C for 30 min (as was sample B) and then annealed at 300°C for 50 h. In this sample, annealed far below T_g for a prolonged time, only reversible structural relaxation was significantly observed [1, 17].

A comparison of the changes in the Mössbauer parameters between samples A and B provides information about the irreversible structural relaxation, and a comparison between samples B and C clarifies the changes in the Fe-site surroundings due to the reversible structural relaxation.

4. Results

The Mössbauer absorption spectra at $300\ \text{K}$ for samples A, B and C are shown in Fig. 1. The spectra are composed of six broadened and overlapping lines having no fine structure. The shapes of these spectra are typical of ferromagnetic metallic glasses containing Fe atoms. These spectra indicate that the samples annealed at 475°C and 300°C hold the amorphous state and any crystalline phase is not included. The amorphous states of samples A, B and C were also confirmed by the XRD analyses. Each Mössbauer spectrum was fitted by a sum (i.e. by overlapping) of five independent kinds of six-line hyperfine splittings with Lorentzian profiles. This fitting method, of course, does not mean that only five kinds of Fe sites

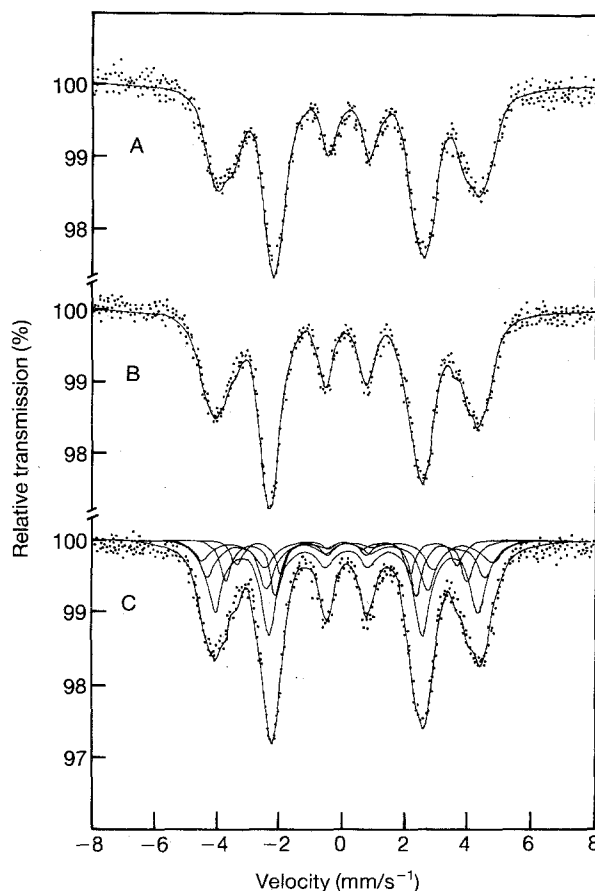


Figure 1 Mössbauer absorption spectra at $300\ \text{K}$ for the $(\text{Co}_{0.75}\text{Fe}_{0.25})_{75}\text{Si}_{10}\text{B}_{15}$ metallic glass. The solid lines are fitted curves. A, B and C are samples A, B and C.

with different magnetic hyperfine fields are present in this metallic glass. The magnetic hyperfine field, H_i , of Fe sites in Fe-based metallic glasses is naturally distributed; this means that numerous Fe sites with different H_i values, or that the distribution of Fe-site surroundings such as the Gaussian distribution, have to be considered, in principle, in the analyses of the Mössbauer spectra. However, the Mössbauer spectra for Fe-based metallic glasses can also be well fitted even by using a limited number of Fe sites with different H_i -values [19, 20]. Since the Mössbauer spectra for samples A, B and C are very similar, the fitting method adopted in this study is considered to be sufficient to compare the differences in Fe-site surroundings in these samples.

It is well known that the intensity ratio of the Mössbauer peaks in the six-line hyperfine splittings depends on the angle between the direction of the incident γ -rays and the angle of the magnetic hyperfine fields (i.e. the direction of the magnetization). In this study, the incident γ -rays are perpendicular to the ribbon plane. If the incident γ -rays and the magnetization are perpendicular, the intensity ratio of $I_{1,6}:I_{2,5}:I_{3,4}$ is 3:4:1, where I_{ij} is the intensity of the i th and j th Mössbauer peaks from the left. As examined in detail by Ito *et al.* [21], the intensity ratio in the Mössbauer peaks for the $(\text{Co}_{0.94}\text{Fe}_{0.06})_{74.5}\text{Si}_{13.5}\text{B}_{12}$ metallic glass was 3:3.9:1, meaning that the magnetization axes are almost completely in the ribbon plane. It has been well confirmed that the magnetization axes in transition-metal/metalloid metallic glasses are almost within the ribbon plane. Thus, in the present study, the fittings of the Mössbauer spectra shown in Fig. 1 were performed by assuming the intensity ratio 3:4:1 for each six-line hyperfine splitting.

Good-quality fitting curves for samples A, B and C are shown in Fig. 1. In sample C, five kinds of six-line hyperfine splittings with different Mössbauer parameters are shown as an example. First the results will be described of the changes in the distributions in the Mössbauer parameters and then the correlations among them will be described. The relative intensity of Fe sites having different H_i -values in samples A, B and C are shown in Fig. 2. It is seen that the distributions of H_i in samples B and C are narrow compared with sample A. Further, by annealing sample B at 300 °C for 50 h, the populations of the Fe sites with low H_i -values around 220 and 240 kOe decrease and conversely those with the relatively high H_i -values of 260 and 275 kOe increase. The relative intensities of Fe sites having different isomer shifts, δ_{IS} , in samples A, B and C are shown in Fig. 3. It is clear that the δ_{IS} -values in the annealed samples are much smaller than those in the as-quenched sample and the distribution of δ_{IS} becomes narrower in the sample order A, B and C. The relative intensities of Fe sites having different quadrupole splittings, Δ_{QS} , in samples A, B and C are shown in Fig. 4. The distribution profiles of Δ_{QS} for these three samples are clearly different. In particular, the distribution tends to separate into two parts with negative or positive Δ_{QS} -values. In Fig. 4, two parts are designated as region-I and region-II.

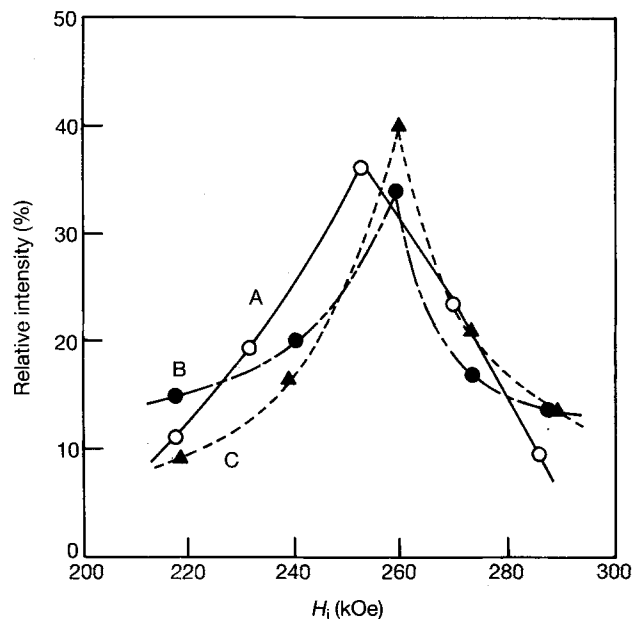


Figure 2 Relative intensities of various Fe sites with different magnetic hyperfine fields, H_i , in the $(\text{Co}_{0.75}\text{Fe}_{0.25})_{75}\text{Si}_{10}\text{B}_{15}$ metallic glass. A, B and C are samples A, B and C.

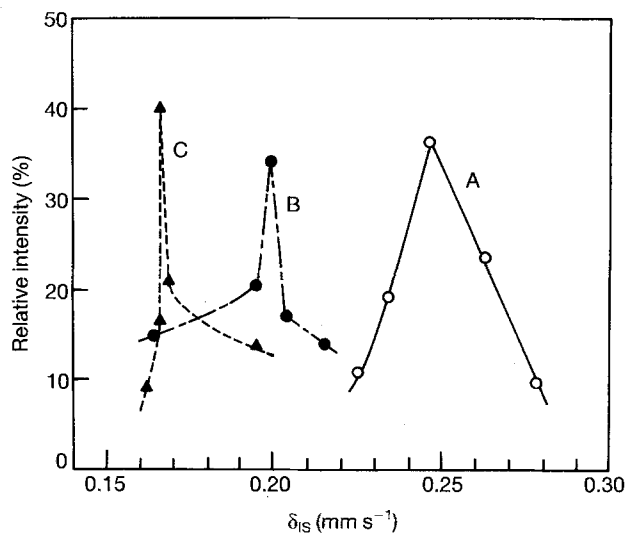


Figure 3 Relative intensities for various Fe sites having different isomer shifts, δ_{IS} , in the $(\text{Co}_{0.75}\text{Fe}_{0.25})_{75}\text{Si}_{10}\text{B}_{15}$ metallic glass. A, B and C are samples A, B and C.

The mean values, $\langle H_i \rangle$, of the magnetic hyperfine field of Fe atoms with five kinds of different surroundings in samples A, B and C were calculated by the following equation:

$$\langle H_i \rangle = \sum_n (H_i)_n P_n \quad (1)$$

where $(H_i)_n$ and P_n are the values of H_i for Fe sites having different surroundings and the relative intensity in each six-line hyperfine splitting. The mean values, $\langle \delta_{\text{IS}} \rangle$, of the isomer shift and those of the quadrupole splitting, $\langle \Delta_{\text{QS}} \rangle$, were also obtained in a similar way. The relationships between $\langle \delta_{\text{IS}} \rangle$ and $\langle H_i \rangle$ and between $\langle \Delta_{\text{QS}} \rangle$ and $\langle H_i \rangle$ are given in Fig. 5. The Fe sites with large values of $\langle H_i \rangle$ have small values of $\langle \delta_{\text{IS}} \rangle$. A similar relationship between $\langle H_i \rangle$ and $\langle \delta_{\text{IS}} \rangle$

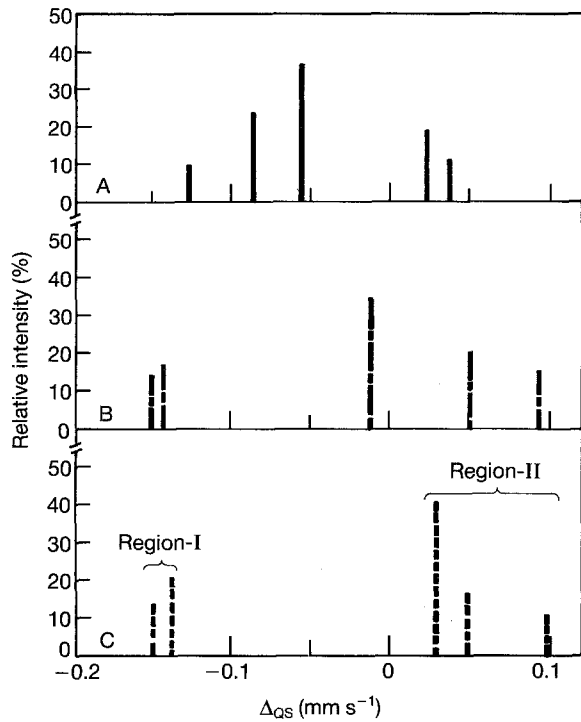


Figure 4 Relative intensities for various Fe sites having different quadrupole splittings, Δ_{QS} , in the $(Co_{0.75}Fe_{0.25})_{75}Si_{10}B_{15}$ metallic glass. A, B and C are samples A, B and C.

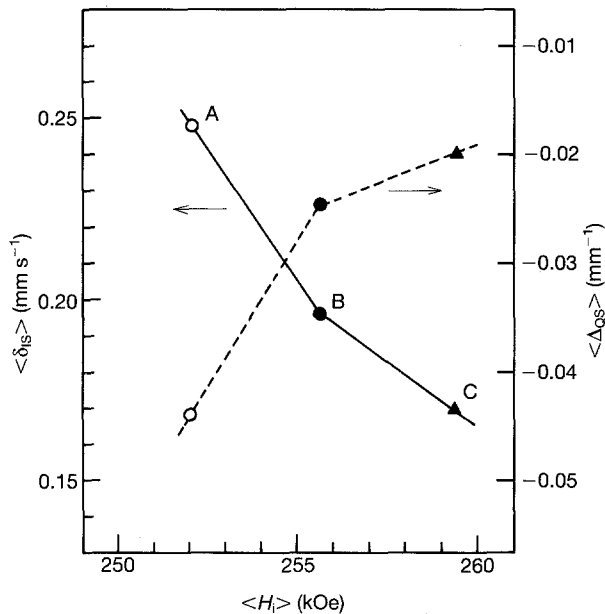


Figure 5 Correlations among the mean magnetic hyperfine field, $\langle H_I \rangle$, the mean isomer shift, $\langle \delta_{1s} \rangle$, and the mean quadrupole splitting, $\langle \Delta_{QS} \rangle$, for Fe sites in the $(Co_{0.75}Fe_{0.25})_{75}Si_{10}B_{15}$ metallic glass. A, B and C are samples A, B and C.

has also been reported for Fe_xB_{100-x} and $Ni_{80-x}Fe_xSi_{10}B_{10}$ metallic glasses [22, 23]. The values of $\langle \Delta_{QS} \rangle$ for samples A, B and C are all negative. Panek *et al.* [24] have also reported that the values of Δ_{QS} for $(Fe_{1-x}Co_x)_{83}B_{17}$ metallic glasses are negative for most of the compositions. It is seen that Fe sites with large values of $\langle H_I \rangle$ have small absolute values of $\langle \Delta_{QS} \rangle$. The relationship between $\langle \delta_{1s} \rangle$ and $\langle \Delta_{QS} \rangle$ is shown in Fig. 6. Some values of δ_{1s} and Δ_{QS} in $(Fe_{1-x}Co_x)_{83}B_{17}$ metallic glasses reported by Panek

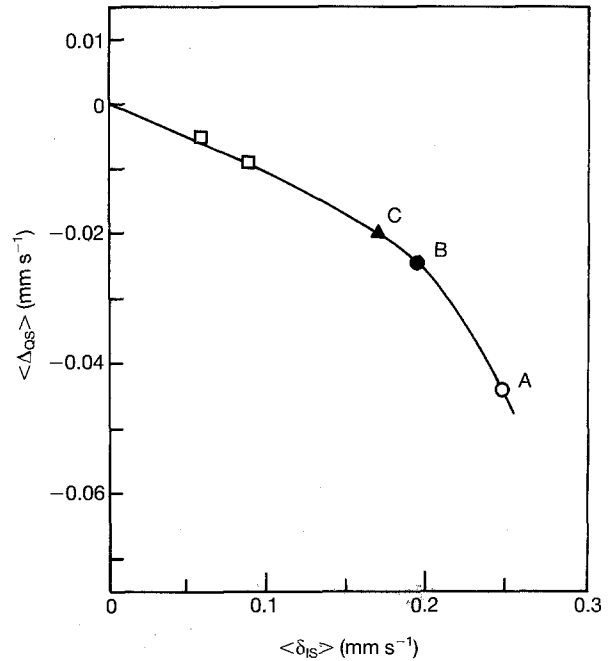


Figure 6 Correlation between the mean isomer shift $\langle \delta_{1s} \rangle$ and the mean quadrupole splitting, $\langle \Delta_{QS} \rangle$ for Fe sites in the $(Co_{0.75}Fe_{0.25})_{75}Si_{10}B_{15}$ metallic glass. A, B and C are samples A, B and C. (\square) Data for $(Fe_{1-x}Co_x)_{83}B_{17}$ metallic glass reported by Panek *et al.* [24].

et al. [24] are also shown in Fig. 6. A very close correlation between $\langle \delta_{1s} \rangle$ and $\langle \Delta_{QS} \rangle$ is observed. The results shown in Figs 2 to 6 indicate that not only a reduction in the fluctuations of Fe-site surroundings but also a large change in the electronic state of Fe atoms occur due to structural relaxation in the $(Co_{0.75}Fe_{0.25})_{75}Si_{10}B_{15}$ metallic glass.

5. Discussion

First, it is worth describing the general features of the Mössbauer parameters, H_I , δ_{1s} and Δ_{QS} , in metallic glasses containing Fe atoms, and also the general features of the electronic structure and magnetism of transition metal (TM)-metalloid (M) metallic glasses briefly. The magnetic hyperfine field of Fe atoms is known to be a measure of the electron spin density. That is, the value of H_I is determined mostly by the magnetic moment of Fe atoms. This moment, of course, is greatly affected by the interaction between the Fe atom and its surroundings. The isomer shift depends primarily on the difference between the electron charge density at the Fe nuclei in an absorber and that in an emitter; that is, the isomer shift is proportional to the density of s-like electrons. For example, an increase in δ_{1s} for Fe atoms means a decrease in the s-like electron density at the Fe nucleus in an absorber. In Fe-B metallic glasses [22, 23] or Fe-Si crystalline alloys [25], the mean value of H_I decreases with increasing B or Si content, and conversely the mean value of δ_{1s} increases. Generally, Fe atoms with high mean H_I -values tend to have small mean δ_{1s} -values. When an Fe site has a low symmetry, an electric-field gradient will result in an electric quadrupole moment of the Fe nucleus, causing a splitting of

the nuclear levels. In TM–M glasses, a large amount of metalloid atoms are inevitably included, and it is obvious that the presence of TM–M bondings is one of the most important origins of electric-field gradients. The fluctuation in the length and angle of TM–M bondings will cause electric-field gradients at a Fe site and, consequently, will produce a distribution in Δ_{QS} and an asymmetrical pattern in the Mössbauer spectrum. The behaviours of the changes in Δ_{QS} due to the structural relaxation will, particularly, shed some important lights on the rearrangements of metalloid atoms.

For most TM–M glasses, the average value of the magnetic moment per TM atom decreases with increasing M content and depends on the type (Si, B, P, Ge) of the M atom present. These observations were interpreted by the charge-transfer model (donor model) [26]. In this model, the decrease of the magnetic moment was explained by electron transfer from M atoms to the d-band of TM atoms. However, many authors have demonstrated that the charge-transfer model is not applicable to the TM–M glasses [27]. Instead of the charge-transfer model, the covalent-bonding model has been introduced to explain the magnetic properties of TM–M glasses and has been strongly supported by various theoretical and experimental arguments [28–31]. The covalent bonding between TM and M atoms, which means the p–d hybridization of the d-states of TM atoms and the p-states of M atoms, causes the delocalization of some of the magnetic d-states and, in consequence, a reduction of the magnetic moment [31]. It is clear that the covalent bonding between TM and M atoms in TM–M glasses such as Co–Fe–Si–B metallic glasses plays a decisive role in the thermal stability, diffusion behaviours and, of course, the structure of metallic glasses.

5.1. Comparison between samples A and B

Now, the results of the Mössbauer spectra are discussed and some conclusions are drawn about the microscopic mechanism of structural relaxation in the $(Co_{0.75}Fe_{0.25})_{75}Si_{10}B_{15}$ metallic glass.

The metallic glasses prepared by rapid-quenching techniques involve frozen-in excess free volume. In structural relaxation, reduction and redistribution of frozen-in excess free volume occur, and, consequently, a very small increase in density of within about 0.6% is observed [32]. The annihilation of the frozen-in excess free volume in as-quenched metallic glasses is usually completed by annealing at or near the glass-transition temperature. It is obvious that a large amount of frozen-in excess free volume is included in sample A (as-quenched glass), and it is considered that this excess free volume is almost annihilated in sample B annealed at near T_g [1]. The structural relaxation of as-quenched glasses would cause not only densification but also rearrangements of the constituent atoms. In particular, in metallic glasses containing several kinds of transition metal and metalloid atoms, it would be expected that many atomic rearrangements occur. In other words, the environments of Fe

sites in Co–Fe–Si–B metallic glasses (i.e. the numbers of Co, Si and B atoms surrounding Fe atoms) would naturally change due to annealing at near T_g .

As shown in Figs 2 and 3, the distributions of H_1 and δ_{IS} in sample B is narrow compared with those in sample A. In particular, the narrowing of the distribution of δ_{IS} in sample B is remarkable, and the decrease in δ_{IS} due to the structural relaxation is very large. The H_1 -value with the strongest relative intensity in sample B is around 260 kOe, but in sample A it is around 250 kOe. As shown in Fig. 4, the values of Δ_{QS} tend to separate into two parts due to the first annealing at 475 °C, although they are still widely distributed. These results clearly demonstrate that the fluctuation of Fe-site surroundings in the as-quenched $(Co_{0.75}Fe_{0.25})_{75}Si_{10}B_{15}$ metallic glass (sample A) decrease due to the annealing at near T_g . In this case, the reduction of the fluctuation of Fe sites would arise from both the densification and the rearrangements among all the constituent atoms.

One of the most effective atomic rearrangements, which causes a large change in the electronic state of Fe atoms, would be the behaviours of metalloid atoms (Si, B). Unfortunately, the short-range structure of Co–Fe–Si–B metallic glasses has not been clarified at the present time. Gaskell [33] has suggested that a basic structural unit in $Pd_{80}Si_{20}$, and other TM–M metallic glasses with about a $TM_{75}M_{25}$ composition, is mainly a trigonal prism with TM_3M composition. It has now been demonstrated that the short-range structure of TM–M metallic glasses can be sufficiently explained using a stereochemically defined structure model such as Ni_3B and Fe_3B but not using the dense-random-packing model of hard spheres (the so-called Bernal model) [20, 34–38]. In the chemically defined structure model, the directional covalent bonding between TM and M atoms plays an intrinsic role in the short-range structure. Komatsu *et al.* [1] have proposed, from the compositional dependence of the resistivity changes during the structural relaxation, that the short-range-ordered structure in the $(Co_{0.75}Fe_{0.25})_{75}Si_{10}B_{15}$ metallic glass annealed at far below T_g corresponds to the atomic arrangement of a $(Co, Fe)_3(Si, B)$ type. Its short-range structure is shown schematically in Fig. 7. In the as-quenched glass, it is expected that the arrangements of Si and B atoms are more random and widely distributed than in the structure shown in Fig. 7. The random distribution of Si and B atoms would result in larger distributions of H_1 , δ_{IS} and Δ_{QS} than is the case for random distribution of Fe and Co atoms only. Chien *et al.* [22] reported that the isomer shift in the Fe–B system decreases largely in the order FeB , Fe_2B and Fe_3B . The extreme narrowing of δ_{IS} in sample B clearly demonstrates that the site positions of Si and B atoms in the short-range structure are well defined and their randomness is small. The behaviour of the changes in Δ_{QS} also strongly support the belief that the rearrangements of Si and B occur during annealing. It can, therefore, be concluded that the most significant atomic rearrangement during the first annealing of the as-quenched glass at near T_g is the rearrangement of Si and B atoms from a random occupation to a well-

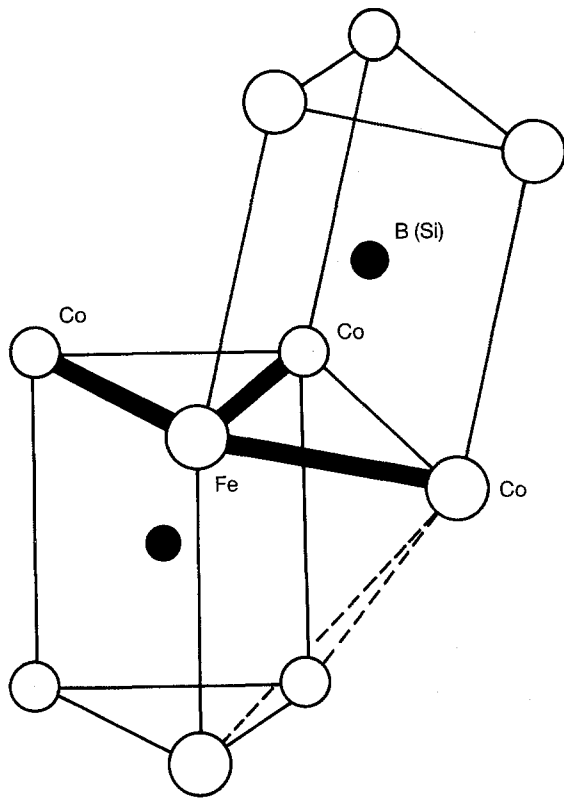


Figure 7 An arrangement of trigonal prismatic units $(\text{Co}, \text{Fe})_3(\text{Si}, \text{B})$ with a metalloid at the centre: (●), Si, B. They are surrounded by transition-metal atoms: (○) Co, Fe. In this structure model, the Co-Fe pairs shown are formed.

defined position in a short-range-ordered structure. The rearrangements of Fe and Co atoms would, of course, occur during the annealing at near T_g . The origin of the separation into two parts in Δ_{QS} has not been well interpreted at this moment, but this tendency implies that two apparently different surroundings, resulting in two different quadrupole splittings of Fe nuclear levels, are mainly present. The inclusion of two kinds of metalloid atoms, Si and B, might be one reason for the distribution in Δ_{QS} .

The present results show clearly that the distribution of Fe-site surroundings becomes narrow largely due to the irreversible structural relaxation or TSRO and that the mean magnetic hyperfine field of Fe atoms increases. The shift towards higher H_i due to TSRO, i.e. due to the annealing of as-quenched glasses at near or below T_g , has been observed in other metallic glasses such as $\text{Fe}_{74}\text{Co}_4\text{Si}_9\text{B}_{13}$ [18] and Fe-B [35, 39]. Ok and Morrish [40] have reported that the atomic ordering in $\text{Fe}_{82}\text{Si}_6\text{B}_{12}$ metallic glass increases during the structural relaxation and this atomic ordering is the origin of the small increases in H_i . The tendency in the change in H_i in samples A and B of $(\text{Co}_{0.75}\text{Fe}_{0.25})_{75}\text{Si}_{10}\text{B}_{15}$ metallic glass obtained in the present study is very consistent with those in the other metallic glasses above.

5.2. Comparison between samples B and C

Even in sample C, the narrowings of the distributions of H_i and δ_{IS} and the shift towards higher $\langle H_i \rangle$ and the decrease in $\langle \delta_{\text{IS}} \rangle$ were clearly observed as shown in

Figs 2 and 3, indicating that distinct rearrangements among constituent atoms occur during the annealing at 300 °C. Further, it is seen that the values of Δ_{QS} in sample C separate clearly into two parts, i.e. region-I and region-II. However, it should be pointed out that the magnitudes of the changes in H_i , δ_{IS} and Δ_{QS} between samples B and C are considerably smaller than those between samples A and B. This means that the degree of atomic rearrangements in sample C is smaller than that in sample B. It is worth remembering that reversible structural relaxation occurs in sample C only, i.e. reversible atomic rearrangements [1]. That is, the present results demonstrate that some atomic rearrangements towards more-ordered short-range structure occur due to the reversible structural relaxation. For the reasons which follow, it is reasonable to assume that the mechanism of reversible structural relaxation corresponds mainly to the short-range ordering and disordering between Co and Fe atoms, as proposed by Komatsu *et al.* [1, 17]. (i) The degree of the reversible structural relaxation in $(\text{Co}_{1-x}\text{Fe}_x)_{75}\text{Si}_{10}\text{B}_{15}$ metallic glasses depends strongly on the Co/Fe ratio [1]. (ii) The covalent bonding between TM and M atoms is not isotropic but is highly directional, meaning that the activation energy for the change in the positions of M atoms would be large and thus it would be very hard for M atoms to move at far below T_g . (iii) In the chemically defined structure model, M atoms are surrounded by TM atoms in a well-defined short-range-ordered structure, and the structure of metallic glasses is composed of random arrangements of short-range-ordered structure. This means that the amount of free volume around M atoms is much smaller than that around TM atoms. Indeed, the activation energy, E_a , for diffusion of TM atoms such as Fe ($E_a = 2.0$ eV in $\text{Fe}_{40}\text{Ni}_{40}\text{P}_{14}\text{B}_6$) in TM-M glasses is generally much smaller than those of M atoms such as Si ($E_a = 2.8$ eV in $\text{Fe}_{82}\text{Si}_6\text{B}_{12}$) and B ($E_a = 3.6$ eV in $\text{Fe}_{40}\text{Ni}_4\text{B}_{20}$) [41–43].

If only the rearrangements between Co and Fe atoms occur in sample C, what effect will be expected on the electronic state of Fe atoms? Generally, the low-temperature annealing at far below T_g in the fully stabilized ferromagnetic TM (Fe, Co, Ni)-M glasses causes the increase in the Curie temperature [3, 44–46], meaning that the magnetic interactions between different TM atoms becomes strong due to the reversible structural relaxation. Further, it should be pointed out that the magnetic hyperfine field of the Fe nucleus in the crystalline Fe-Co system increases with increasing Co content up to 30 at %, which is similar to the so-called Slater-Pauling curve for the saturation magnetic moment [47]. According to Bardos [48], the magnetic moments of the ordered Fe-Co crystalline alloys are larger than those of the disordered (quenched) alloys. These results clearly indicate that the magnetic moment of Fe atoms in Fe-Co alloys is mainly determined by the number of cobalt atoms locating at the nearest-neighbour distance. That is, the chemical ordering between Fe and Co atoms plays a decisive role in the magnetic moment of Fe atoms in Fe-Co crystalline alloys. There-

fore, if the chemical ordering between Co and Fe atoms occurred even in Co-Fe-Si-B metallic glasses, we can expect the increase in the magnetic moment of Fe atoms and thus the increase in $\langle H_i \rangle$ and the decrease in $\langle \delta_{IS} \rangle$. Further, the chemical ordering between Co and Fe atoms would produce the reduction of the distributions of H_i and δ_{IS} . The results shown in Figs 2, 3 and 5 clearly support the above model. The chemical ordering between Co and Fe atoms in the metallic glasses is termed the chemical short-range ordering between Co and Fe atoms.

Gibbs and Hygate [49] have suggested that a change in CSRO will in general cause a change in TSRO by the shearing component of a migratory atomic jump and by the size differences of the migrating species. Since the sizes of Fe and Co atoms are almost the same, the overall topological changes such as the decrease in atomic distances during the chemical ordering between Fe and Co atoms would be negligibly small. However, as shown in Fig. 4, the change in Δ_{QS} has clearly occurred in the sample C. This result might mean that small changes in the positions of Si and B atoms occur during the reversible structural relaxation in addition to the atomic rearrangements between Co and Fe atoms.

The relative change in $\langle H_i \rangle$ between samples B and C, $(\langle H_i \rangle_C - \langle H_i \rangle_B) / \langle H_i \rangle_B$, is 1.48%, as shown in Fig. 5. The relative change in the electrical resistivity between these two samples, which was estimated from the data reported by Komatsu *et al.* [1, 17], is 0.96% and is close to the value (1.48%) in $\langle H_i \rangle$. It is worth remembering that the percentage of the property changes due to reversible structural relaxation is usually around 1% or less [49]. In general, the degree of short-range-order parameter in AB binary alloys is described by a Warren-Cowley parameter (WCP), or the chemical short-range order in metallic glasses can be estimated from the concentration/concentration structure factor shown by Bhatia and Thornton [50]. At least, the small values in the relative change in $\langle H_i \rangle$ and electrical resistivity between samples B and C suggest that the change in the WCP or in the atomic-pair-distribution function would be small. Indeed, the confirmation of atomic rearrangements due to the CSRO in metallic glasses through direct diffraction experiments such as pulsed neutron scattering is extremely difficult [7].

Good correlations among $\langle H_i \rangle$, $\langle \delta_{IS} \rangle$ and $\langle \Delta_{QS} \rangle$ have been observed in samples A, B and C, as shown in Figs 5 and 6. These results clearly demonstrate that the short-range ordering among Co, Fe, Si and B atoms occurs during both irreversible and reversible structural relaxation, and particularly Fe-site environments in the samples annealed at near and below T_g are well defined. Further, it has been clarified that both the values of the isomer shift and of the quadrupole-splitting approach gradually to zero due to the structural relaxation and consequently the value of the magnetic hyperfine field increases. In the present study, the microscopic mechanism in the structural relaxation of the $(\text{Co}_{0.75}\text{Fe}_{0.25})_{75}\text{Si}_{10}\text{B}_{15}$ metallic glass has been confirmed for the first time. The information obtained through the Mössbauer-effect ex-

periments could be applied effectively to the study on the structural relaxation in other transition-metal/metalloid metallic glasses.

6. Conclusions

The changes in Fe-site surroundings during the irreversible and reversible structural relaxation in the $(\text{Co}_{0.75}\text{Fe}_{0.25})_{75}\text{Si}_{10}\text{B}_{15}$ metallic glass were examined by Mössbauer-effect measurements on Fe atoms. The following results were obtained.

1. Narrowing of the distributions in H_i and δ_{IS} and separation into two parts in Δ_{QS} due to the structural relaxation were observed. The shift towards higher values in $\langle H_i \rangle$ and the decrease in $\langle \delta_{IS} \rangle$ were also observed. Very close correlations among $\langle H_i \rangle$, $\langle \delta_{IS} \rangle$ and $\langle \Delta_{QS} \rangle$ were obtained.

2. The present study strongly supports the irreversible-structural relaxation correspondence to the topological short-range ordering being mainly due to the ordering of Si and B atoms from random distributions to well-defined positions and the reversible structural relaxation arising mainly from the chemical short-range ordering between Co and Fe atoms.

The metallic glass used in the present study is very suitable for the study of the microscopic mechanism of reversible structural relaxation, which is still one of the main subjects in metallic glasses.

Acknowledgements

We thank M. Ichikawa for technical assistance of the Mössbauer-effect measurements. We also thank Dr K. Nakajima of Tohoku University, Dr S. Okamoto of Nagaoka College of Technology and Professor K. Matusita of Nagaoka University of Technology for help throughout the present study.

References

1. T. KOMATSU, S. SATO and K. MATUSITA, *Acta Metall.* **34** (1986) 1899.
2. T. KOMATSU, K. FUJITA, K. MATUSITA, K. NAKAJIMA and S. OKAMOTO, *J. Appl. Phys.* **68** (1990) 2091.
3. R. YOKOTA, M. TAKEUCHI, T. KOMATSU and K. MATUSITA, *ibid.*, **55** (1984) 3037.
4. A. INOUE, T. MASUMOTO and H. S. CHEN, *J. Mater. Sci.* **19** (1984) 3953.
5. E. BALANZAT, J. T. STANLEY, C. MAIRY and J. HILLAIRET, *Acta Metall.* **33** (1985) 785.
6. T. EGAMI, *Mater. Res. Bull.* **13** (1978) 557.
7. A. VAN DEN BEUKEL and S. RADELAAR, *Acta Metall.* **31** (1983) 419.
8. T. KOMATSU, *Res Mechanica* **31** (1990) 263.
9. A. BOHONYEY and L. F. KISS, *J. Phys. Condens. Matter* **3** (1991) 4523.
10. R. BRUNING, Z. ALTOUNIAN and J. O. STROM-OLSEN, *J. Appl. Phys.* **62** (1987) 3633.
11. G. HYGATE and M. R. J. GIBBS, *J. Phys. F*: **17** (1987) 815.
12. R. BRUNING and J. O. STROM-OLSEN, *Phys. Rev. B* **41** (1990) 2678.
13. Y. WU, W. DMOWSKI, T. EGAMI and M. E. CHEN, *J. Appl. Phys.* **61** (1987) 3219.
14. T. KOMATSU and K. MATUSITA, in Proceedings of the Symposium on Magnetic Properties of Amorphous Metals, edited by A. Hernando, V. Madurga, C. Sanchez-Trujillo and M. Vazquez (North-Holl and, Amsterdam, 1987) p. 74.

15. T. KOMATSU, S. SATO and K. MATUSITA, *J. Non-Cryst. Solids* **95-96** (1987) 985.
16. *Idem.*, *ibid.* **91** (1987) 52.
17. T. KOMATSU, K. IWASAKI, S. SATO and K. MATUSITA, *J. Appl. Phys.* **64** (1988) 4853.
18. E. PLIPCZUK and M. KOPCEWICZ, *J. Mater. Sci. Lett.* **9** (1990) 565.
19. C. L. CHIEN and R. HASEGAWA, *Phys. Rev. B* **16** (1977) 3024.
20. T. KEMENY, I. VINCZE and B. FOGARASSY, *ibid.* **20** (1979) 476.
21. A. ITO, E. TORIKAI, S. MORIMOTO, K. SHIKI and M. KUDO, in Proceedings of the 4th International Conference on Rapidly Quenched Metals, edited by T. Masumoto and K. Suzuki (Japanese Institute of Metals, 1982) p. 1101.
22. C. L. CHIEN, D. MUSSER, E. M. GYORGY, R. C. SHERWOOD, H. S. CHEN, F. E. LUBORSKY and J. L. WALTER, *Phys. Rev. B* **20** (1979) 283.
23. R. J. POLLARD, Z. S. WRONSKI and A. H. MORRISH, *ibid.*, **29** (1984) 4864.
24. T. PANEK, H. W. BERGMANN, U. LUFT and I. LANGFORD, in Proceedings of the 4th International Conference on Rapidly Quenched Metals, edited by T. Masumoto and K. Suzuki (Japanese Institute of Metals, 1982) p. 537.
25. M. B. STEARNS, *Phys. Rev.* **129** (1963) 1136.
26. K. YAMAUCHI and T. MIZOGUCHI, *J. Phys. Soc. Jpn.* **39** (1975) 541.
27. R. C. O'HANDLEY, in Amorphous metallic alloys, edited by F. E. Luborsky (Butterworths, Boston, 1983) p. 257.
28. J. W. ALLEN, A. C. WRIGHT and G. A. N. CONNELL, *J. Non-Cryst. Solids* **42** (1980) 509.
29. R. P. MESSMER, *Phys. Rev. B* **23** (1981) 1616.
30. B. W. CORB, R. C. O'HANDLEY and N. J. GRANT, *J. Appl. Phys.* **53** (1982) 7728.
31. Z. M. STADNIK and G. STROINK, *J. Non-Cryst. Solids* **99** (1988) 233.
32. T. KOMATSU, K. MATUSITA and R. YOKOTA, *ibid.* **85** (1986) 358.
33. P. H. GASKELL, *ibid.* **32** (1979) 207.
34. I. VINCZE and F. VAN DER WOUDE, *ibid.* **42** (1980) 499.
35. R. OSHIMA and F. E. FUJITA, *Jpn. J. Appl. Phys.* **20** (1981) 1.
36. P. PANISSOD, I. BAKONYI and R. HASEGAWA, *Phys. Rev. B* **28** (1983) 2374.
37. K. SUZUKI, T. FUKUNAGA, F. ITOH, and N. WATANABE, in Proceedings of the 5th International Conference on Rapidly Quenched Metals, edited by S. Steeb and H. Warlimont (North-Holland, Amsterdam, 1985) p. 479.
38. T. KOMATSU, Y. TANAKA, R. YOKOTA and K. MATUSITA, *J. Mater. Sci.* **22** (1987) 2185.
39. S. M. CHERMISIN and A. YU. DUDKIN, *Solid State Commun.* **74** (1990) 673.
40. H. N. OK and A. H. MORRISH, *Phys. Rev. B* **22** (1980) 3471.
41. P. VALENTA, K. MAIER, H. KRONMULLER and K. FREITAG, *Phys. Status Solidi (b)* **106** (1981) 129.
42. R. W. CAHN, J. E. EVETTS, J. PATTERSON, R. E. SOMEKH and C. K. JACKSON, *J. Mater. Sci.* **15** (1980) 702.
43. F. E. LUBORSKY and F. BACON, in Proceedings of the 4th International Conference on Rapidly Quenched Metals, edited by T. Masumoto and K. Suzuki (Japanese Institute of Metals, 1982) p. 561.
44. T. KOMATSU, K. MATUSITA and R. YOKOTA, *J. Mater. Sci.* **20** (1985) 3271.
45. T. KOMATSU and K. MATUSITA, *J. Mater. Sci. Lett.* **5** (1986) 311.
46. Z. Y. SHIN, J. X. HONG, Y. Y. ZHANG and S. A. HE, *J. Appl. Phys.* **67** (1990) 3655.
47. C. E. JOHNSON, M. S. RIDOUT, T. E. CRANSHAW and P. E. MADSEN, *Phys. Rev. Lett.* **6** (1961) 450.
48. D. I. BARDOS, *J. Appl. Phys.* **40** (1969) 1371.
49. M. R. J. GIBBS and G. HYGATE, *J. Phys. F* **16** (1986) 809.
50. A. B. BHATIA and D. E. THORNTON, *Phys. Rev. B* **2** (1974) 3004.

Received 19 June 1992

and accepted 20 April 1993